Autonomous growth of spatially localized supramolecular hydrogel through emergence of autocatalytic ability

Jennifer Rodon Fores, Miryam Criado-Gonzalez, Alain Chaumont, Alain Carvalho, Christian Blanck, Marc Schmutz, Fouzia Boulmedais, Pierre Schaaf, Loïc Jierry

Autonomous growth of spatially localized supramolecular hydrogel through emergence of autocatalytic ability

Jennifer Rodon Fores[a], Miryam Criado-Gonzalez[a,b], Alain Chaumont[c], Alain Carvalho[a], Christian Blanck[a], Marc Schmutz[a], Fouzia Boulmedais[a], Pierre Schaaf[a,b]* and Loïc Jierry[a]*

[a] Dr. J. Rodon Fores, Dr. M. Criado-Gonzalez, A. Carvalho, C. Blanck, Dr. M. Schmutz, Dr. F. Boulmedais, Prof. Dr. P. Schaaf, Prof. Dr. L. Jierry
Université de Strasbourg, CNRS
Institut Charles Sadron (UPR22)
23 rue du Loess, BP 84047, 67034 Strasbourg Cedex 2 (France)
E-mail: schaaf@unistra.fr
ljierry@unistra.fr

[b] Dr. M. Criado-Gonzalez, Prof. Dr. P. Schaaf
Institut National de la Santé et de la Recherche Médicale
INSERM Unité 1121
11 rue Humann, 67085 Strasbourg Cedex (France)
and
Université de Strasbourg
Faculté de Chirurgie Dentaire
8 rue Sainte Elisabeth 67000 Strasbourg (France)

[c] Dr. A. Chaumont
Université de Strasbourg
Faculté de Chimie, UMR7140
1 rue Blaise Pascal, 67008 Strasbourg Cedex (France)

Supporting information for this article is given via a link at the end of the document.

Abstract: Autocatalysis and self-assembly are key processes in developmental biology and are involved in the emergence of life. In the last decade both features were extensively investigated by chemists with the final goal to design synthetic living systems. Herein, we describe the autonomous growth of a self-assembled soft material, *i.e.* a supramolecular hydrogel, able to sustain its own formation through an autocatalytic mechanism not based on any template effect and emerging from a peptide (hydrogelator) self-assembly. A domino sequence of events starts from an enzymatically triggered peptide generation followed by their self-assembly into catalytic nanofibers inducing and amplifying their production over time, resulting in a 3D hydrogel network. A cascade is initiated by traces (10^{-18} M) of a trigger enzyme which can be localized allowing for a spatial resolution of this autocatalytic buildup, an essential condition to fulfil on the route toward further cell mimic designs.

Introduction

Living systems can be considered as highly complex sets of chemical reactions coupled to a variety of self-assembly processes which work in concert both spatially and temporally in a self-sustained way.[1,2] Even if most of individual molecular processes taking place in this orchestra can now be mimicked synthetically in solution, the future key challenge is to couple them in a spatiotemporal way through compartmentalization and leading to multi-scale organizations in a metabolism-like pathway.[3,4] In mimicking living organization, a first step addressed by the chemical community was the design of chemical systems allowing for self-replication property.[5-11] This is characterized by a template effect based on discrete numbers of building blocks capable of recognition to replicate their own structure, playing thus the role of seed of their own formation.[12] First examples were provided by RNA self-replicators.[13] This lies in connection with the RNA world, a hypothetical stage of the emergence of life on earth.[14] Different strategies using peptides or purely synthetic compounds have also emerged. This is the case of self-replicating helicoidal peptides where the replicating peptide acts as a template for peptide fragments and catalyzes their ligation.[15] Self-replication can also be driven by the dynamic self-assembly of the replicator molecules. This allows sorting specific compounds out from a mixture through a dynamic combinatorial library approach.[16,17] Recently, the design of macroscopic 3D materials from a template-triggered effect has been reported, *i.e.* supramolecular hydrogel which represents a first important step toward mimicking living systems *de novo*.[18,19] Confinement of this self-replication process is another aspect to take into account in order to get compartmentalization which allow for spatial localization and enclosure of chemical components and reactions. In this field, it has been shown that the interface of aggregates of amphiphilic compounds can produce their own constituting component.[9,20] More recently, a phase separation between precursors have been shown as responsible of both the localized replicator formation and destruction.[21]

Autonomous self-sustained processes can not only be obtained by self-replication but also by another autocatalytic process.[12] Here we present the autonomous and spatially localized buildup of a soft material thanks to a catalytic ability raising from its own network formation, efficient enough to ensure the transformation of a large scope of various substrates. As self-replication, this autocatalysis is highly interesting for artificial living system development since many biological processes show this kind of autocatalytic features.[22] To date, the design of materials displaying a growth based on this kind of autocatalysis has never been reported. In our case, a self-sustained process ensures a continuous growth of a material. We have designed an original amphiphilic diester heptapeptide **HE²** (**H** for hydrogelator, **E** for ester, Figure 1a), lacking catalytic activity, but once both ester groups are hydrolyzed the remaining hydrogelator **H** self-

assembles leading to a supramolecular hydrogel having highly efficient esterase-like activity.[23] The self-sustained growth of the catalytic hydrogel is initiated by generating traces of **H** in the chemical system *in situ* thanks to an enzymatic action. The choice of an enzyme trigger is motivated by several advantages: (*i*) it is the most efficient class of catalysts allowing a quick production of **H** and an accurate regulation of its concentration, initiating the gelation process using very few enzymes; (*ii*) enzymes can be spatially localized through grafting methods providing localization of **H** generation[24] and thus of the hydrogel growth.[25,26] This is an essential requirement to fulfil for further development in the cell mimic design where compartmentation of different events needs to be controlled; (*iii*) because amphiphilic hydrogelators are low soluble compounds, the use of an enzymatic trigger allows the introduction of enzymatically-cleavable hydrophilic groups.[27] We have thus chemically modified the **H** heptapeptide denoted **HP²** (**P** for phosphate) by introducing two phosphate groups, highly sensitive to alkaline phosphatase (**AP**). The water-soluble precursor **HP²** was first dissolved at small amount and when **AP** was added, its biocatalytic action released the hydrogelator **H** which self-assembled and initiated the self-sustained growth mechanism (Figure 1b).

Figure 1. (a) Chemical structures of the hydrogelator heptapeptides H and precursor peptides HP2 and HE2; (b) Schematic representation of the autocatalytic production of the hydrogelator **H** initiated from **HP²** and **AP** and self-sustained through the hydrolysis of the diester **HE²**. The precursor **HP²** is enzymatically dephosphorylated by **AP** leading to the self-assembly of the hydrogelator **H**. From the resulting assembly emerges an esterase-like activity efficient enough to hydrolyze **HE²** in **H**, self-sustaining thus the growth of the catalytic material.

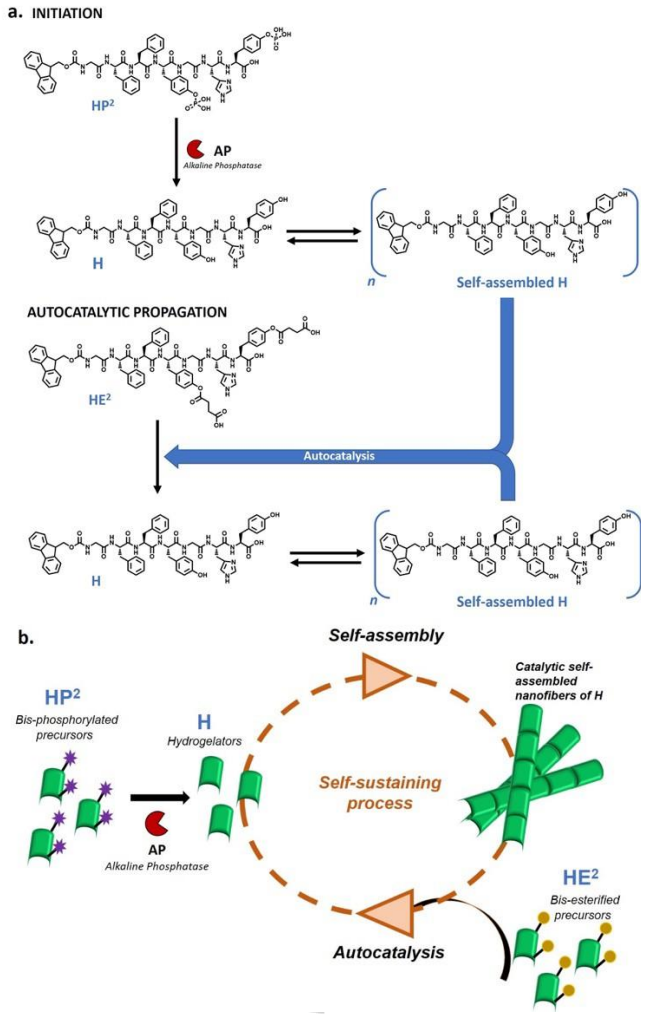

Results and Discussion

Self-assembly of peptides H catalyzes the production of H through the hydrolysis of the precursors HE². Recently we have shown that heptapeptides **H**, *i.e.* Fmoc-GFFYGHY, exhibit a catalytic activity when they are self-assembled resulting in hydrogel formation which catalyzes efficiently the hydrolysis of a large panel of non-activated esters,[23] a feature barely reported in the literature for self-assembled catalytic systems.[28-32] Indeed, all classes of ester are catalytically transformed in their corresponding carboxylic acid using this catalytically-active supramolecular hydrogel (CASH). Based on this exceptional efficiency, we have designed the precursor peptide **HE²** (SI, Section 2): in the peptide sequence of **H**, phenol groups of the two tyrosine residues were esterified with succinic anhydride to get a water-soluble **HE²** precursor. This heptapeptide is pre-assembled in water but fully dispersed in DMSO according to ^{1}H NMR analyses. When a solution of **HE²** (200 µL, 0.76 mM) is diffusing within the CASH of **H**, HPLC monitoring shows a full conversion of **HE²** in **H** in less than 24 hours highlighting the ability of the **H** self-assembly to catalyze the production of its own building blocks (Figure S1). Intermediates **HE** peptides have not been detected and identified during the conversion of **HE²** in **H**.

Autocatalytic H hydrogel growth initiated by an enzyme. In order to initiate the self-assembly process, one needs to introduce another precursor that transforms into **H** by an orthogonal reaction to the hydrolysis of esters. Following the same strategy described just above, we have modified the tyrosine residues of the **H** peptide with phosphate groups to get the following precursor Fmoc-GFF*p*YGH*p*Y named **HP²** (Figure 1a, Section 2 in SI). **HP²** is a water-soluble peptide which does not self-assemble and exhibits no catalytic activity. The amount of **H** peptide released from **HP²** can be tuned using **AP** because this enzymatic action allows a total generation of **H**. We thus mixed **HP²**, **AP** and **HE²** by keeping the concentration of **HE²** constant at 7.6 mM and by decreasing the concentrations of both **HP²** and **AP** from 790, 79, 7.9, 0.79 µM and 5.9, 0.59, 0.059, 0.0059 µM respectively. We followed the conversion of **HE²** in **H** over time by HPLC (Figures 2a and S2). The concentration of 10 mg/mL for **HE²** was chosen because it corresponds to the critical gelation concentration (CGC) of **H**.[23] In all cases, the *in situ* generation of **H** is formed with a decreasing kinetic when the concentrations of **AP** and **HP²** are reduced: for the lower concentration of **AP** and **HP²**, (5.9 nM and 0.79 µM respectively), the transformation of **HE²** into **H** starts significantly after 27 hours and then the transformation accelerates in a manner like a nucleation and growth process (Figure 2a). After 72 hours, full conversion of **HE²** in **H** is obtained. This can be interpreted as follows: the enzyme **AP** transforms **HP²** in **H**, which self-assembles and then starts catalyzing the transformation on **HE²** peptides into **H** which further self-assemble leading to a self-sustained growth of the self- assembly process. The formation of **H** shows first a lag period followed by an exponential growth because the **H** assembly accelerates the rate of its production, therefore acting as a typical autocatalyst.[12]

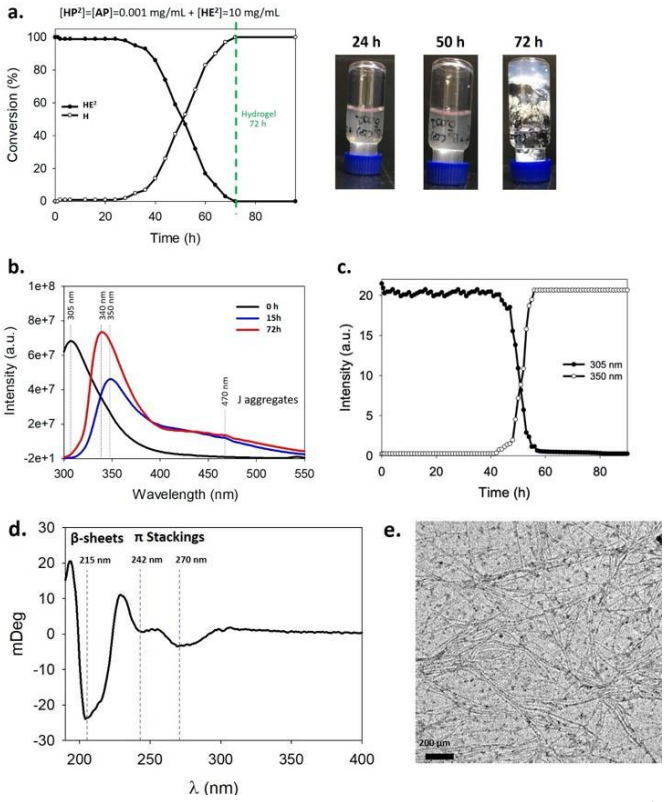

Figure 2. (**a**) (*left*) HPLC monitoring at 254 nm of the conversion of **HE²** in **H** over time in presence of **HP²** (0.79 µM), **AP** (5.9 nM) and **HE²** (7.6 mM) to the initial time; (*right*) Inverted test tube's pictures of the vial after 24, 50 and 72 hours; (**b**) Emission fluorescence intensity measurements at t=0, 15 and 72 h of the **HP²** (0.79 µM), **AP** (5.9 nM) and **HE²** (7.6 mM) mixture when the solution is excited at 290 nm.; (**c**) evolution of the fluorescence intensity measured at 305 nm and 350 nm. All experiments were performed with an initial solution of 5.9 nM of **AP** and 0.79 µM of **HP²** and 7.6 mM of **HE²**; (**d**) CD measurements and (**e**) TEM image of the resulting diluted hydrogel formed from **AP** (5.9 nM) and **HP²** (0.79 µM) and **HE²** (7.6 mM). Corresponding HT data of the CD spectra is given in SI.

Characterization of the H self-assembly and of the resulting supramolecular hydrogel. We followed the self-assembly of **H** peptides by fluorescence spectroscopy ($\lambda_{ex.}$=290 nm). A model experiment was performed by mixing 0.79 µM of **HP²** and **AP** (5.9 nM) with 7.6 mM of **HE²**. After 12 hours the maximum band emission at 305 nm, characteristic of Fmoc groups, starts to shift toward roughly 350 nm and a band at 450-
460 nm appears due to the presence of J-aggregates, a typical behavior of the molecular self-assembly of Fmoc peptides containing phenylalanines (Figure 2b).[33] By measuring the evolution of the emission fluorescence at 350 nm, one can follow the self-assembly kinetics of **H** which occurs 15 hours before the detection of **H** by HPLC (Figure 2c), probably due to the higher sensitivity of fluorescence emission than UV detection. The secondary structure of **H** self-assembly was determined by CD spectroscopy. One observes a peak at 215 nm attributed to β-sheets structures and two peaks at 242 nm and 270 nm attributed to the π-stacking between the aromatic rings (Figure 2d). This self-assembly is being expressed at the nanometer scale through the formation of several micrometer long nanofibers (φ ~ 6-7 nm for thinner fibers) as observed by TEM (Figure 2e). After 72 hours, an inverted tube test shows the formation of hydrogel. Such material was characterized by rheology showing a G' value (7 kPa at 1 Hz) significantly higher than G" (800 Pa at 1 Hz) (Figure 3a). At a constant frequency of 1 Hz the gel appears stable by increasing the strain up to 1%. Molecular dynamic simulation (MDS) of 16 hydrogelators **H** in aqueous solution lead to an equilibrated state after ~ 0.1 ms highlighting antiparallel β-sheet structures in agreement with CD measurements and π stacking of Fmoc groups. By analogy with catalytic sites well identified in esterase enzymes, histidine is considered as the main residue involved in the hydrolytic mechanism. The efficiency of this activity is based on the nucleophilicity feature of one nitrogen of the imidazole ring. Hydrogen bonding between imidazoles allows to increase the nucleophilicity of the nitrogen and thus increase the esterase activity through a cooperative catalytic effect.[34] Thus, the localization of histidine residues relatively close to each other indicates potential catalytic pocket. Through MDS, two "pockets" constituted of three and six histidines forming hydrogen networks are located externally to the fiber-like assembly of **H** having a roughly 3 nm diameter (Figures 3b, S3).

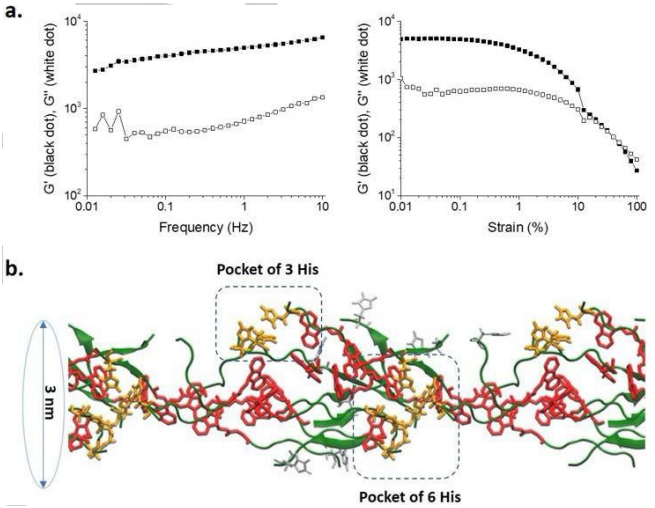

Figure 3. Rheological study of the **H** hydrogel prepared from **HE²** (7.6 mM), **AP** (5.9 nM), and **HP²** (0.79 µM). (**a**) Evolution of storage modulus G' and the loss modulus G" with frequency at a strain of 1% (*left*) and with strain at a given frequency of 1 Hz (*right*); (**b**) Molecular dynamics of hydrogelators **H** showing a fiber-like spatial arrangement through 3D periodic boundary conditions. Green arrows represent the β-sheet structures, Fmoc moieties are in red, histidine residues involved in a hydrogen network are in yellow, the others in grey.

Serial transfer experiments demonstrate the self-sustained growth of H self-assembly. To prove the capacity of the **H** hydrogel to catalyze the production of **H** from the diester precursor **HE²** hydrolysis, we performed serial transfer experiments: after **H** hydrogelation, we extracted a piece (~100 mg) of the **H** hydrogel (1 mM), inserted it in a PBS buffer (pH 7.4) and vortexed this heterogeneous mixture to get a viscous-like solution of H self-assembled nanofibers. Then, an aliquot of this solution was added to a **HE²** precursor solution in order to get a molar ratio 8/1 between **HE²** and **H** respectively (total concentration in **H** after **HE²** hydrolysis: 7.6 mM. The transformation of **HE²** into **H** was monitored by HPLC for 100 hours (Figure 4a). The formation of **H** is detected at t = 25h and its concentration increases over time following a sigmoid curve. After 60 h, **HE²** is fully converted into **H** and a new hydrogel is obtained. When a piece is taken from this **H** hydrogel and this

experiment is repeated a second time, the same behavior is observed. Identical results are obtained in a third experiment from a piece of the **H** hydrogel taken from the second hydrogelation experiment. This operation was thus repeated three times. It proves that self-assemblies composed of **H** peptides catalyze the transformation of **HE²** into **H** leading to the formation of a hydrogel. A fourth run was performed where a smaller extracted piece from the third hydrogel was used to reach a molar ratio of 8/0.001 (instead of 8/1) between **HE²** and **H** respectively. Conversion kinetics of **HE²** into **H** is slower and gel forms only after 120 hours.

Attomolar traces of AP initiates the autocatalytic self-assembly process. In principle, only a single biomacromolecule of **AP** can produce **H** hydrogelators from **HP²**, which self-assemble and thus catalyze their own production from **HE²** hydrolysis. Realistically, this kind of *butterfly effect* can only have sense with a minimum number of **AP**. Keeping a ~1/10 000 ratio between **HP²** (0.79 µM) and **HE²** (7.6 mM) respectively, the concentration of **AP** was gradually decreased from nanomolar up to zeptomolar and the self-assembly of **H** was followed through the emission of fluorescence at 350 nm over time (Figures 4b, S4). This emission remains close to a nil value for an initial time laps that increases when the **AP** concentration decreases: ~ 40 hours ([**AP**]=10 nM), ~78 hours ([**AP**]=1 pM), ~90 hours ([**AP**]=1 fM) and ~ 138 hours ([**AP**]=1 aM). Then, the fluorescence emission intensity increases exponentially and correlatively the fluorescence emission measured at 305 nm, characteristic of **HE²**, decreases up to zero. This time laps must correspond to the time required to transform enough **HP²** into **H** to induce self-assembled structures able to catalyze the hydrolysis of **HE²** into **H** and thus autocatalyze the self-assembly process. One can point out that in all experiments where the concentrations of **AP** were decreased up to a concentration of 1 aM, one always switches from 0% to 100 % of conversion of **HE²** into **H**, resulting in hydrogelation. This is in accordance with the expectation for an autocatalytic process. One zeptomolar of **AP** was also tested but no formation of **H** was detected even after one week, as observed in absence of **AP**. Considering the 200 µL in which all these experiments were carried out, one attomolar of **AP** corresponds to ~120 biomacromolecules: this number highlights the considerable amplification process taking place in this chemical system to get the soft matter formation.

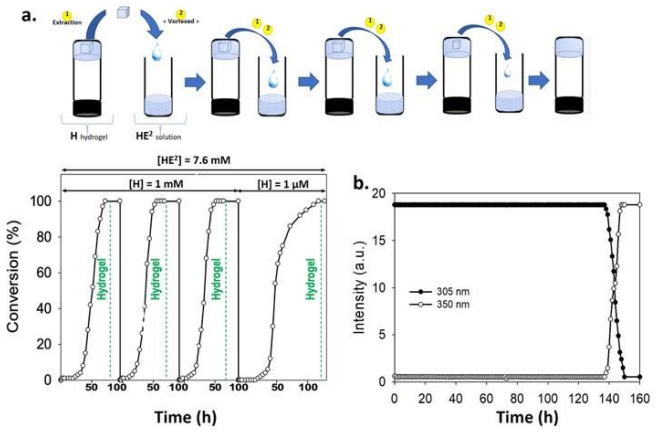

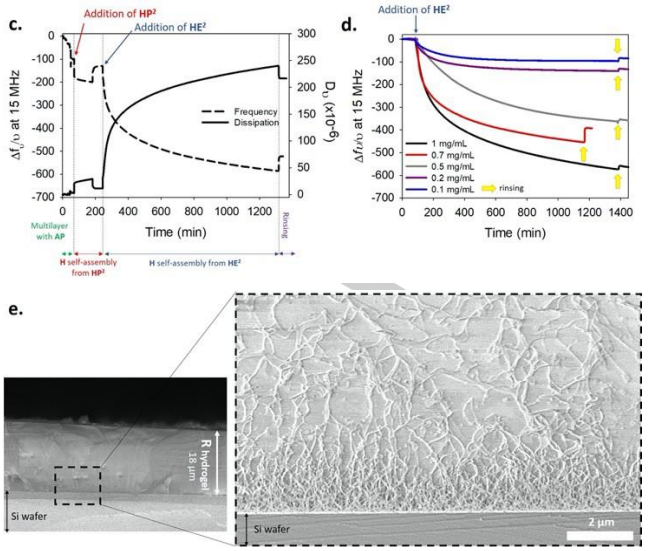

Figure 4. (**a**) Serial transfer experiments starting with a **HE²** solution (7.6 mM) and a piece of seeding gel containing 1 mM or 1 µM of **H** to initiate the autocatalytic self-assembly process; (**b**) Fluorescence emission intensity measurements monitored over time at 305 and 350 nm when excited at 290 nm for the following solution : **HP²** (7.9 10^{-4} mM), **HE²** (7.6 mM) and **AP** (1 aM); (**c**) Evolution of the QCM-D signals, frequency shift (full line) and dissipation (dotted line) corresponding to the 3rd harmonic of the autocatalytic self-assembly initiated at the crystal surface modified by a PEI-$(PSS/PAH)_2$-**AP** multilayer. The multilayer is first brought in contact with a **HP²** solution at 0.79 µM followed by a rinsing step and then in contact with a **HE²** solution at 0.76 mM or (**d**) at 0.53, 0.38, 0.15 and 0.076 mM. (**e**) *Cryo*-SEM images of the localized self-assembled **H** hydrogel grown from the **AP**-modified silicium wafer.

Spatial localization of the self-sustained hydrogel growth. Because the **H** peptide self-assembly process is initiated enzymatically, its spatial control can be realized through the localization of the enzymes at defined areas which requires their immobilization.[24,35,36] To get a proof of principle, the **AP** was electrostatically adsorbed onto a flat substrate (quartz or silicon wafer) using the polyelectrolyte multilayer film strategy.[37] A thin film (20 nm) constituted of 2.5 alternations of poly(ethylene imine) (PEI) and sodium poly(styrene sulfonate) (PSS) allows the electrostatic adsorption of **AP** on the top leading to the following PEI-$(PSS/PEI)_2$-**AP** nanoarchitecture. This enzymatically-active multilayer was then brought in contact with a **HP²** solution at low concentration (0.79 µM) for 110 minutes and then rinsed thoroughly. The evolution of the deposited mass on the substrate was followed using a quartz crystal microbalance with dissipation (QCM-D) (Figure 4c). The decreasing of the crystal frequency indicates a deposition of matter and a thin thickness value of 6 nm is calculated (SI, section 5), meaning that few seeding-fibers of **H** are exposed on the top of the film as observed by AFM (Figure S5). Then, this modified surface was put in contact with a solution of **HE²** (0.76 mM) leading to a strong decrease of the frequency shift. This evolution takes place at the same time as a huge increase of the dissipation factors. Both behaviors are symptomatic of hydrogel formation.[23, 25, 26] It must be noted that despite that the **HE²** concentration is 10 times lower than the CGC needed in the bulk to obtain a hydrogel, hydrogelation occurs from the **AP**-modified surface. The amount of hydrogel formed from the enzymatic multilayer is depending on the concentration of **HE²** solution brought in contact with the film: decreasing this concentration from 0.76, 0.53, 0.38, 0.15 and 0.076 mM

decreases concomitantly the mass of hydrogel generated according to QCM-D measurements (Figure 4d). When 0.76 mM of **HE²** is used, the thickness of the resulting hydrogel layer reaches ~18 µm according to *cryo*-SEM analysis (Figure 4e). The enzymatic formation of **H** nanofibers and their catalytic action toward **HE²** self-sustained the continuous **H** assembly through a cascade of events that must be realized in this sequential order. Indeed, when **HE²** is used instead of **HP²** no frequency shift is measured by QCM-D. Moreover, in absence of **AP** in the multilayer, **HP²** is not hydrolyzed and the following contact with **HE²** does not lead to any hydrogel formation (Figure S6).

A gradient of nanofibers network nucleates and grows perpendicularly from the surface. Cryo-SEM images of the cross-section of the substrate along the z axis shows a full coverage by the H supramolecular hydrogel exclusively from the enzymatically-active multilayer film (Figure 4e). More strikingly, a network of entangled nanofibers is mainly perpendicularly oriented to the substrate. We can also observe that the self- assembled H nanofibers density is high in close vicinity with the surface and decreases towards the solution. This gradient of fibers density from the surface to the environment agrees with a higher concentration of H at the interface due to the localization of enzymes confining there hydrogelators H from HE2.

Conclusion

Autocatalytic biological processes are complex phenomena proceeding from the molecular scale and beyond, involving spatial localizations of 3D organizations communicating with one another. Rare contributions have been reported about the autonomous growth of self-assembled materials, *i.e.* hydrogel formed in the bulk, based on a self-templated approach of a dynamic combinatorial library.[18,19] Here, we have designed a chemical system based on the peptide sequence of a hydrogelator **H**, *i.e.* Fmoc-GFFYGHY, which leads to an esterase- like hydrogel that catalyzes the formation of its own building blocks. The hydrogel formed is able to hydrolyse a large panel of esters, but its formation cannot start by itself: it must be initiated by presence of self-assemblies of **H**, at least. This can be achieved by triggering the formation of hydrogelators **H** through an enzymatic reaction that is orthogonal to the reaction catalyzed by the self-assembled material itself. Traces of the precursor **HP²** (0.79 µM) as well as an attomolar quantity of enzymes **AP** appear sufficient to initiate the growth process, similarly to sequential steps observed in biological systems. Biocatalytic initiation of the process is of great interest because it allows localizing the gel formation by localizing the enzymes. We also find that the spatial localization of the enzymes leads to localized self-assembly processes at hydrogelator concentrations that are at least ten times lower than the CGC to get a supramolecular hydrogel in the bulk. This is due to spatial confinement of enzymes producing locally an out-of-equilibrium area where hydrogelators are concentrated enough to give birth to the material.[38] It is also found that the fibers composing the self-assembled nanoarchitecture initiated at a surface present a preferential orientation perpendicular to the surface and a gradient of fibers density from the surface to the top.[39] This represents an interesting aspect regarding the anisotropic properties of biological tissues emerging from orientated internal organizations. This feature appears to be shared with others self-assembled processes initiated from catalytic surfaces.[40] The future challenge will be to develop localized self-assembly processes mimicking cellular behavior, operating thus in the context of coupled mixed processes occurring sequentially in time and at various space-scales. The reduction of the initiation area to the nanometric size on a surface is also an important requirement to carry out the compartmentalization of theses chemical systems.

Acknowledgements

This work was financially supported by *the Agence Nationale de la Recherche* (project "EASA" ANR-18-CE06-0025-03), the *Fondation pour la Recherche en Chimie* (FRC, project number PSC-005), the Labex *Chimie des Systèmes Complexes* (CSC), and Institut Carnot-MICA (project POLYSPRAY). J.R.F. acknowledges the FRC and Labex CSC (project number PSC-016) for her PhD fellowship. The ICS microscopy platform and the ICS characterization platform are acknowledged. AC acknowledges the HPC-Unistra for GPU time. Muhammad Haseeb Iqbal is acknowledged for his technical help in the AFM measurements.

Conflict of interest

The authors declare no competing financial interest.

Keywords: Autocatalysis • Peptide Self-assembly • Supramolecular Chemistry • Hydrogels • Surface Chemistry

[1] A. Pross in *Oxford University Press*: Oxford, U.K., **2012**.
[2] P. Schwille, J. Spatz, K. Landfester, E. Bodenschatz, S. Herminghaus, V. Sourjik, T. J. Erb, P. Bastiaens, R. Lipowsky, A. Hyman, P. Dabrock, J.-C. Baret, T. Vidakovic-Koch, P. Bieling, R. Dimova, H. Mutschler, T. Robinson, T.-Y. D. Tang, S. Wegner, K. Sundmacher, *Angew. Chem., Int. Ed.* **2018**, *57,* 13382−13392; *Angew. Chem.* **2018**, *130*, 13566-13577.
[3] B. Liu, C. G. Pappas, J. Ottelé, G. Schaeffer, C. Jurissek, P. F. Pieters, M. Altay, I. Marić, M. C. A. Stuart, S. Otto, *J. Am. Chem. Soc.* **2020**, 142, 4184-4192.
[4] J. Boekhoven, W. E. Hendriksen, G. J. M. Koper, R. Eelkema, J. H. van Esch, *Science* **2015**, *349*, 1075-1079.
[5] S. Kamioka, D. Ajami, J. Rebek, *Proc. Natl. Acad. Sci. U. S. A.* **2010**, *107*, 541−544.
[6] N. Vaidya, M. L. Manapat, I. A. Chen, R. Xulvi-Brunet, E. J. Hayden, N. Lehman, *Nature* **2012**, *491*, 72 −77.
[7] E. Kassianidis, D. Philp, *Angew. Chem., Int. Ed.* **2006**, *45*, 6344− 6348; *Angew. Chem., Int. Ed.* **2006**, *118*, 6492-6496.
[8] D. H. Lee, J. R. Granja, J. A. Martinez, K. Severin, M. R. Ghadiri, *Nature* **1996**, *382*, 525−528.
[9] A. J. Bissette, B. Odell, S. P. Fletcher, *Nat. Commun.* **2014**, *5*, 4607.
[10] T. A. Lincoln, G. F. Joyce, *Science* **2009**, 323, 1229−1232.
[11] G. Ashkenasy, R. Jagasia, M. Yadav, M. R. Ghadiri, *Proc. Natl. Acad. Sci. U. S. A.* **2004**, *101*, 10872−10877.
[12] A. J. Bissette, S. P. Fletcher, *Angew. Chem., Int. Ed.* **2013**, *52*, 12800–12826; *Angew. Chem.* **2013**, *125*, 13034–13061.
[13] G. von Kiedrowski, *Angew. Chem., Int. Ed.* **1986**, *25*, 932−935; *Angew. Chem.***1986**, *98*, 932−934.
[14] G. F. Joyce, J. W. Szostak, *Cold Spring Harbor Perspect. Biol.* **2018**, doi: 10.1101/cshperspect.a034801.
[15] R. Issac, Y.-W. Ham, J. Chmielewski, *Curr. Opin. Struct. Biol.* **2001**, *11*, 458-463.

[16] D. Komaromy, M. Tezcan, G. Schaeffer, I. Maric, S. Otto, *Angew. Chem., Int. Edit.* **2017**, *56*, 14658-14662; *Angew. Chem.* **2017**, 129, 14850-14854.
[17] B. Bartolec, M. Altay, S. Otto, *Chem. Commun.* **2018**, *54*, 13096-13098.
[18] J. Li, J. M. A. Carnall, M. C. A. Stuart, S. Otto, *Angew. Chem., Int. Ed.* **2011**, *50*, 8384−8386; *Angew. Chem.* **2011**, *123*, 8534-8536.
[19] J. Li, I. Cvrtila, M. Colomb-Delsuc, E. Otten, S. Otto, *Chem. - Eur. J.* **2014**, *20*, 15709−15714.
[20] P. A. Bachmann, P. L. Luisi, J. Lang, *Nature* **1992**, *357*, 57-59.
[21] I. Colomer, S. M. Morrow, S. P. Fletcher, *Nat. Commun.* **2018**, *9*, 2239.
[22] C. J. Gadgil, B. D. Kulkarni, AIChE Journal **2009**, *55*, 556-562.
[23] J. Rodon Fores, M. Criado-Gonzalez, A. Chaumont, A. Carvalho, C. Blanck, M. Schmutz, C. A. Serra, F. Boulmedais, P. Schaaf, L. Jierry *Angew. Chem., Int. Ed.* **2019**, *58*, 18817-18822; *Angew. Chem.* **2019**, *131*, 18993-18998.
[24] R. J. Williams, A. M. Smith, R. Collins, N. Hodson, A. K. Das, R. V. Ulijn, *Nat. Nanotechnol.* **2009**, *4*, 19 −24.
[25] C. Vigier-Carrière, T. Garnier, D. Wagner, P. Lavalle, M. Rabineau, J. Hemmerlé, B. Senger, P. Schaaf, F. Boulmedais, L. Jierry, *Angew. Chem., Int. Ed.* **2015**, *54*, 10198–10201; *Angew. Chem.* **2015**, *127*, 10336-10339.
[26] J. Rodon Fores, M. L. Martinez Mendez, X. Mao, D. Wagner, M. Schmutz, M. Rabineau, P. Lavalle, P. Schaaf, F. Boulmedais, L. Jierry, *Angew. Chem., Int. Ed.* **2017**, *56*, 15984–15988; *Angew. Chem.* **2017**, *129*, 16200-10204.
[27] Z. Yang, H. Gu, D. Fu, P. Gao, J. K. Lam, B. Xu, *Adv. Mater.* **2004**, *16*, 1440-1444.
[28] M. O. Guler, S. I. Stupp, *J. Am. Chem. Soc.* **2007**, *129*, 12082–12083.
[29] F. Rodriguez-Llansola, B. Escuder, J. F. Miravet, *J. Am. Chem. Soc.* **2009**, *131*, 11478–11484.
[30] C. M. Rufo, Y. S. Moroz, O. V. Moroz, J. Stöhr, T. A. Smith, X. Hu, W. F. DeGrado, I. V. Korendovych, *Nat. Chem.* **2014**, *6*, 303-309.
[31] N. Singh, K. Zhang, C. A. Angulo-Pachon, E. Mendes, J. H. van Esch, B. Escuder, *Chem. Sci.* **2016**, *7*, 5568–5572.
[32] O. Zozulia, M. A. Dolan, I. V. Korendovych, *Chem. Soc. Rev.* **2018**, *47*, 3621–3639.
[33] A. M. Smith, R. J. Williams, C. Tang, P. Coppo, R. F. Collins, M. L. Turner, A. Saiani, R. V. Ulijn, *Adv. Mater.* **2008**, *20*, 37–41.
[34] S. Bal, K. Das, S. Ahmed, D. Das, *Angew. Chem., Int. Ed.* **2019**, *58*, 244-247; *Angew. Chem.* **2019**, *131*, 250-253.
[35] C. Vigier-Carrière, F. Boulmedais, P. Schaaf, L. Jierry, *Angew. Chem., Int. Ed.* **2018**, *57*, 1448–1456; *Angew. Chem.* **2018**, *130*, 1462–1471.
[36] B. Yang, D. J. Adams, M. Marlow, M. Zelzer, *Langmuir* **2018**, *34*, 15109−15125.
[37] G. Decher, *Science* **1997**, *277*, 1232-1237.
[38] B. Riess, J. Boekhoven, *ChemNanoMat* **2018**, *4*, 710-719.
[39] M. Aono, K. Ariga, *Adv. Mater.* **2016**, *28*, 989–992.
[40] A. G. L. Olive, N. H. Abdullah, I. Ziemecka, E. Mendes, R. Eelkema, J. H. van Esch, *Angew. Chem., Int. Ed.* **2014**, *53*, 4132– 4136. *Angew. Chem.* **2014**, *126*, 4216–4220.

Entry for the Table of Contents

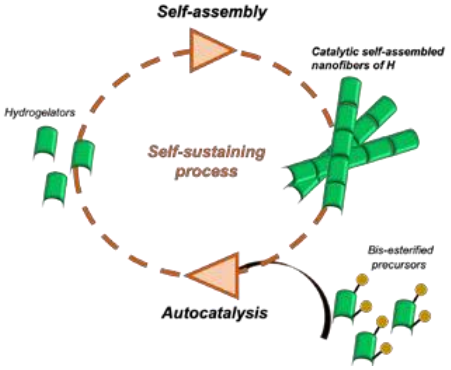

J. Rodon Fores, M. Criado-Gonzalez, A. Chaumont, A. Carvalho, C. Blanck, M. Schmutz, F. Boulmedais, P. Schaaf* and L. Jierry*

Autonomous growth of spatially localized supramolecular hydrogel through emergence of autocatalytic ability

Towards emergence of life: A domino sequence of events starts from traces of enzyme triggering peptide generation followed by their self-assembly into catalytic nanofibers inducing and amplifying their production over time. This self-sustained cycle lead to an autocatalytic self-assembled buildup, an essential condition to fulfil toward further cell mimic designs.